

TRANSMISSION LINE CODE MODELING OF THE PLASMA FLOW SWITCH

P.F. Ottinger
 Naval Research Laboratory, Washington, DC 20375-5000
 P.J. Turchi, D. Conte
 R&D Associates, Alexandria, VA 22314
 J. D. Shipman, Jr.
 Sachs Freeman Associates, Bowie, MD 20716

Abstract

The plasma flow switch (PFS) utilizes the motion of a high density plasma discharge to accumulate and then release magnetic energy at multimegampere, multimegajoule levels.¹ Energy input to a coaxial plasma gun occurs in several microseconds as the annular plasma discharge is accelerated axially along the center conductor. Energy is released to a load in a few hundred nanoseconds as this plasma is expelled off the end of the center conductor. Low density plasma upstream of the axially-moving discharge can limit the flow of electromagnetic power to speeds related to the local Alfvén speed. The wave transit time between the load and the magnetic energy store can compare with the desired energy extraction time. The effects of finite wave speed have been investigated using approximate acoustic analyses.² The present paper utilizes a transmission line code with varying time and impedance elements to model wave transit effects during PFS operation including commutation and load dynamics.

I. Introduction

The PFS utilizes a high density plasma discharge to conduct current while electromagnetic energy is concentrated in an inductive store just upstream of the PFS as illustrated schematically in Fig. 1a. The annular plasma discharge in cylindrical geometry is initiated early in time by driving current through an exploding foil/wire array in vacuum.³ The plasma is accelerated downstream by the axial $\mathbf{j} \times \mathbf{B}$ force and magnetic energy is accumulated in the inductor as the current rises. The plasma mass and plasma gun electrode lengths are chosen such that the plasma moves across an opening gap with a speed of several cm/ μ s when the inductor is fully energized. Multimegampere level currents can be conducted for several microseconds in this fashion, inductively storing energy at the multimegajoule level.

For the purpose of this paper a dynamic imploding foil load is assumed to be located in the opening gap as illustrated in Fig. 1b. As the high density plasma moves across the opening gap the stored energy can be released to the load, however, low density plasma trailing the current sheet limits the flow of the electromagnetic power to speeds related to the local Alfvén speed, v_A . The wave transit time between the load and the magnetic energy store can be comparable with the desired energy extraction time. Typically energy is released on a timescale of a few hundred nanoseconds. This low density plasma results from current contacts at the surfaces, UV-ablation of walls, and Rayleigh-Taylor instability of the upstream boundary of the accelerating current sheet. Because of its low mass, the plasma rapidly expands radially inward into the gap filling the entire volume to the imploding foil. Both the plasma density, n , and the magnetic field, B , in the opening gap are then functions of time with the wave

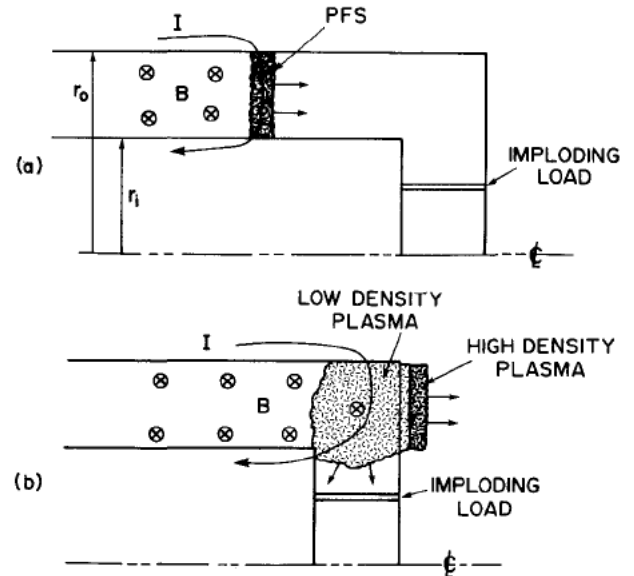


Fig. 1 Schematic of PFS a) run down and b) commutation

speed varying as $v_A \sim B/n^{1/2}$. The effects of finite wave speed during the opening phase of the PFS have been investigated in some detail using approximate acoustic analyses.² For the purposes of this paper, however, it will be assumed that v_A simply increases linearly in time.

The present paper utilizes a transmission line code⁴ with varying time and impedance elements to model PFS operation including commutation and load dynamics. In a transmission line code a circuit element is modeled by a characteristic length or transit time, τ , expressed in seconds and a characteristic impedance, Z , expressed in ohms. The inductance of the element is given by $L = \tau Z$ and the capacitance of the element is given by $C = \tau/Z$. Forward moving voltage waves, V_+ , and backward moving voltage waves, V_- , travel on the transmission line elements with amplitudes determined by the reflection and transmission coefficients at the various junctions of elements. The voltage at any point is given by $V = V_+ + V_-$ and current is given by $I = (V_+ - V_-)/Z$.

During the run-down of the PFS as shown in Fig. 1a, the impedance of the cylindrical transmission line is assumed to be fixed while the length increases as the plasma is accelerated such that $L(t) = \tau(t)Z$. A discussion of how to model this type of transmission line element within the context of the code (described in Ref. 4) is found in Section II. During the commutation phase the physical dimensions of the opening gap do not change, however, the wave transit speed through the low density plasma is much less than the speed of light and also varies with time. This region then is modeled by a fixed inductance, L , and a variable transit time, $\tau(t)$, such that $Z(t) = L/\tau(t)$. A

Report Documentation Page				Form Approved OMB No. 0704-0188	
Public reporting burden for the collection of information is estimated to average 1 hour per response, including the time for reviewing instructions, searching existing data sources, gathering and maintaining the data needed, and completing and reviewing the collection of information. Send comments regarding this burden estimate or any other aspect of this collection of information, including suggestions for reducing this burden, to Washington Headquarters Services, Directorate for Information Operations and Reports, 1215 Jefferson Davis Highway, Suite 1204, Arlington VA 22202-4302. Respondents should be aware that notwithstanding any other provision of law, no person shall be subject to a penalty for failing to comply with a collection of information if it does not display a currently valid OMB control number.					
1. REPORT DATE JUN 1985		2. REPORT TYPE N/A		3. DATES COVERED -	
4. TITLE AND SUBTITLE Transmission Line Code Modeling Of The Plasma Flow Switch				5a. CONTRACT NUMBER	
				5b. GRANT NUMBER	
				5c. PROGRAM ELEMENT NUMBER	
6. AUTHOR(S)				5d. PROJECT NUMBER	
				5e. TASK NUMBER	
				5f. WORK UNIT NUMBER	
7. PERFORMING ORGANIZATION NAME(S) AND ADDRESS(ES) Naval Research Laboratory, Washington, DC 20375-5000				8. PERFORMING ORGANIZATION REPORT NUMBER	
9. SPONSORING/MONITORING AGENCY NAME(S) AND ADDRESS(ES)				10. SPONSOR/MONITOR'S ACRONYM(S)	
				11. SPONSOR/MONITOR'S REPORT NUMBER(S)	
12. DISTRIBUTION/AVAILABILITY STATEMENT Approved for public release, distribution unlimited					
13. SUPPLEMENTARY NOTES See also ADM002371. 2013 IEEE Pulsed Power Conference, Digest of Technical Papers 1976-2013, and Abstracts of the 2013 IEEE International Conference on Plasma Science. Held in San Francisco, CA on 16-21 June 2013. U.S. Government or Federal Purpose Rights License.					
14. ABSTRACT The plasma flow switch (PFS) utilizes the motion of a high density plasma discharge to accumulate and then release magnetic energy at multimegampere, multimegajoule levels.1 Energy input to a coaxial plasma gun occurs in several microseconds as the annular plasma discharge is accelerated axially along the center conductor. Energy is released to a load in a few hundred nanoseconds as this plasma is expelled off the end of the center conductor. Low density plasma upstream of the axially-moving discharge can limit the flow of electromagnetic power to speeds related to the local Alfven speed. The wave transit time between the load and the magnetic energy store can compare with the desired energy extraction time. The effects of finite wave speed have been investigated using approximate acoustic analyses. The present paper utilizes a transmission line code with varying time and impedance elements to model wave transit effects during PFS operation including commutation and load dynamics.					
15. SUBJECT TERMS					
16. SECURITY CLASSIFICATION OF:			17. LIMITATION OF ABSTRACT SAR	18. NUMBER OF PAGES 4	19a. NAME OF RESPONSIBLE PERSON
a REPORT unclassified	b ABSTRACT unclassified	c THIS PAGE unclassified			

detailed discussion of this model is found in Section II of the paper and Section IV of the paper includes a summary of the results of this work.

II. Modeling PFS Run-Down

During the run-down of the PFS, it is assumed that the plasma can be approximated by a thin current carrying annulus of mass, m , which is uniformly accelerated downstream by the $\underline{j} \times \underline{B}$ force. The equation of motion for the annulus is

$$m \frac{d^2 \ell}{dt^2} = Z_f I^2 / 2c, \quad (1)$$

where Z_f is the fixed impedance of the cylindrical transmission line in which the annulus is moving, $I(t)$ is the current, $\ell(t) = c\tau(t)$ is the distance the annulus has traveled and c is the speed of light in vacuum. The instantaneous inductance of the region created by the motion of the PFS is $L(t) = Z_f \tau(t)$. The velocity of the moving annulus, $v(t) = d\ell/dt = c d\tau/dt$, is related to the changing inductance by $dL/dt = Z_f d\tau/dt = (Z_f/c) v(t)$. The kinetic energy imparted to the plasma annulus then is related to the changing inductance through

$$\frac{1}{2} m v^2 = \int \frac{1}{2} \frac{dL}{dt} I^2 dt. \quad (2)$$

The rate of increase of electromagnetic energy stored in the transmission line element then is reduced by the rate of increase of the kinetic energy of the plasma.

In order to model the run-down of the PFS, a transmission line element of fixed impedance, Z_f , and varying length is used. Since numerically the element is an integral number of timesteps or segments long at any given instant, the length $\tau(t)$ of the element changes in discrete steps in accordance with Eq. (1). Between timesteps the length of the element is instantaneously adjusted such that the charge, $Q = CV$, and flux, $\phi = LI$, in the element are conserved. The field energy is not conserved in this case, because kinetic energy is imparted to the plasma. When the element is N timesteps long (i.e. $\tau_p(t) = N\Delta\tau$), the charge and flux in the j^{th} segment of the element at the i^{th} timestep are

$$Q_j^i = \left(\frac{V_{+j}^i + V_{-j}^i}{Z_f} \right) \Delta\tau, \quad j = 1, \dots, N \quad (3)$$

$$\phi_j^i = (V_{+j}^i - V_{-j}^i) \Delta\tau, \quad j = 1, \dots, N \quad (4)$$

where $\Delta\tau$ is the timestep. If between timestep i and timestep $i + 1$, the length of the element is increased from $N\Delta\tau$ to $M\Delta\tau$, then charge and flux are distributed in the M segments by maintaining the shape of the distribution of Q and ϕ along the length of the element as illustrated in Fig. 2. Before the voltage waves are advanced at timestep $i + 1$, the voltage waves on the element are adjusted according to

$$\tilde{V}_{+j}^i = \frac{\tilde{Q}_j^i Z_f}{2\Delta\tau} + \frac{\tilde{\phi}_j^i}{2\Delta\tau}, \quad j = 1, \dots, M \quad (5)$$

$$\tilde{V}_{-j}^i = \frac{\tilde{Q}_j^i Z_f}{2\Delta\tau} - \frac{\tilde{\phi}_j^i}{2\Delta\tau}, \quad j = 1, \dots, M \quad (6)$$

where the tilde over the variable indicate they are the new adjusted variables. Note that reflection and transmission coefficients associated with the

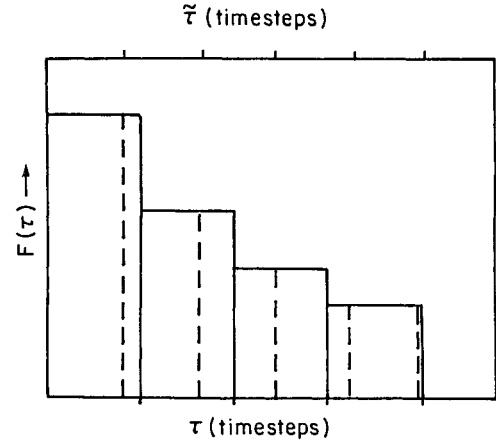


Fig. 2 Illustration of redistribution where solid (dashed) lines divide portion of F in each segment before (after) change in length from τ to $\bar{\tau}$.

transmission line junctions at the two ends of the element are unaltered because Z_f is fixed in this case.

As an example consider the simple circuit shown in Fig. 3. The first element represents a capacitor with $C = \tau_c / Z_c = 10 \mu\text{F}$, the second element is an inductor with $L_s = Z_s \tau_s = 40 \text{ nH}$, and the third element represents a PFS with an initial inductance of $L_p(0) = Z_f \tau_p(0) = 0.5 \text{ nH}$. The circuit is terminated on the left by a large resistance, R_c , to simulate an open circuit and terminated on the right by a short circuit simulating the PFS plasma. The quarter cycle current risetime is $1 \mu\text{s}$ without accounting for the PFS motion and is indicated by the solid curve in Fig. 4a. For a PFS mass of $m = 1.6 \text{ mg}$ and a travel of 10.5 cm or 14 timesteps with $\Delta\tau = 0.025 \text{ ns}$, the current is given by the dashed curve in Fig. 4a and the PFS position is given by the dotted curve. Figure 4b shows the energies stored in the capacitor and in the inductor [i.e. $L_s + L_p(t)$] and the kinetic energy of the PFS. The peak current decreases when a PFS is included in the circuit because of the increased inductance and the energy lost to kinetic energy of the PFS mass.

III. Modeling PFS Current Commutation

As the high density, high speed plasma moves across the opening gap, current is carried by a trailing low density plasma as shown schematically in Fig. 1b. The characteristic speed of the current propagation through such low density plasma is the Alfvén speed which is much less than the speed of light in vacuum. Although the inductance of the gap region, L_1 , is small, the transit time, τ_1 , can be long, and hence the effective impedance, Z_1 , is small. For an imploding foil load this initial transit time can be comparable with the implosion time. However as the magnetic field increases and plasma density decreases, the transit time can significantly decrease, allowing the stored energy to be rapidly released.

In order to model this type of transmission line element, it is assumed that L_1 is fixed and therefore $Z_1(t) = L_1 / \tau_1(t)$. The transit time can be modeled by using appropriate acoustic analysis²,

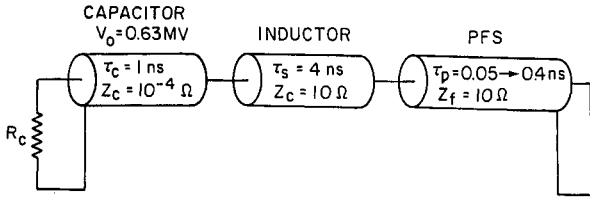


Fig. 3 Circuit for PFS run down.

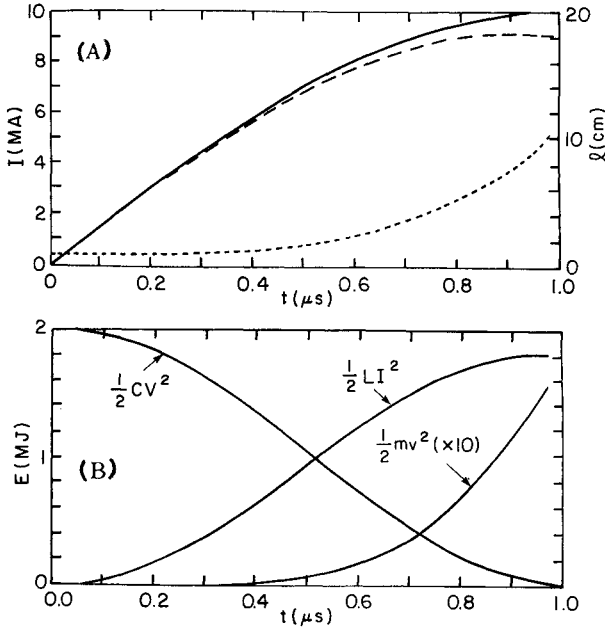


Fig. 4 Plot of a) current with no PFS motion (solid), with PFS motion (dashed) and PFS position (dotted) and b) energy distribution with PFS motion.

however, for simplicity it is assumed here that $\tau_1(t)$ decreases linearly in time from 100 ns to 5 ns in ~ 200 ns. Again numerically the element is an integral number of timesteps or segments long at any instant and thus $\tau_1(t)$ changes in discrete steps. The length is adjusted instantaneously between timesteps. Unlike the case previously discussed where kinetic energy is extracted from the field energy, here the energy in the element is conserved as $Z_1(t)$ and $\tau_1(t)$ vary. When the element is N timesteps long (i.e. $\tau_1(t) = N\Delta\tau$), the forward flowing energy, E_+ , and the backward flowing energy, E_- , in the j th segment of the element at the i th timestep are

$$E_{+j}^i = (V_{+j}^i)^2 \Delta\tau / Z_1(t_i), \quad j = 1, \dots, N \quad (7)$$

$$E_{-j}^i = (V_{-j}^i)^2 \Delta\tau / Z_1(t_i), \quad j = 1, \dots, N \quad (8)$$

where again $\Delta\tau$ is the timestep. If between timestep i and $i+1$, the length of the element is decreased from $N\Delta\tau$ to $M\Delta\tau$, then the forward flowing energy and backward flowing energy is distributed in the M segments in the same manner as discussed previously. Before the voltage waves are advanced at timestep $i+1$, the voltage waves on the element are adjusted according to

$$\tilde{V}_{+j}^i = (\tilde{Z}_1(t_i) \tilde{E}_{+j}^i / \Delta\tau)^{1/2}, \quad j = 1, \dots, M \quad (9)$$

$$\tilde{V}_{-j}^i = (\tilde{Z}_1(t_i) \tilde{E}_{-j}^i / \Delta\tau)^{1/2}, \quad j = 1, \dots, M \quad (10)$$

where $\tilde{Z}_1(t_i) = NZ_1(t_i)/M$ and again the tilde

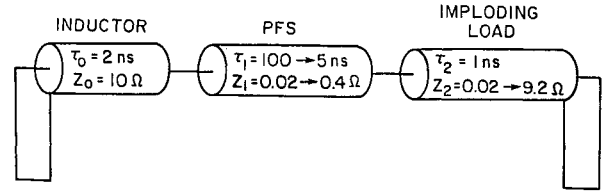


Fig. 5 Circuit for PFS current commutation.

indicates the adjusted variables. In this case care must be taken to preserve the sign of the voltage waves. Since Z_1 changes, the reflection and transmission coefficients associated with the transmission line junctions at the two ends of the element must also be adjusted accordingly.

As an example consider the simple circuit shown in Fig. 5. The first element represents an inductor with $L_0 = Z_0 \tau_0 = 20$ nH, the second element represents the PFS with $L_1 = Z_1(t) \tau_1(t) = 2$ nH, and the third element represents the imploding load with $L_2(t) = Z_2(t) \tau_2(t) = 0.02$ nH and mass per unit length $m/l = 150$ mg/cm. Since the intent here is to study transit time effects on energy transfer, all three elements are initialized carrying 10 MA of current. Most of the energy, however, resides in the storage inductor L_0 . The load is modeled by a simple one timestep long element which has a varying impedance to simulate the varying inductance of the element. The instantaneous inductance (and therefore impedance) of the load is calculated from $L = 2 \times 10^{-7} \ln(r/r(t))$ and adjusted between timesteps using the simple slug model

$$\frac{m}{l} \frac{d^2 r}{dt^2} = - \frac{\mu_0 I^2}{4\pi r}, \quad (11)$$

to determine the load dynamics. The voltage waves are adjusted in order to conserve charge and flux with energy extracted in the form of kinetic energy of the implosion so that

$$\tilde{V}_+^i = \frac{1}{2} [V_+^i (\tilde{Z}_2/Z_2 + 1) + V_-^i (\tilde{Z}_2/Z_2 - 1)] \quad (12)$$

$$\tilde{V}_-^i = \frac{1}{2} [V_-^i (\tilde{Z}_2/Z_2 + 1) + V_+^i (\tilde{Z}_2/Z_2 - 1)] \quad (13)$$

Because Z_2 changes, the reflection and transmission coefficients are also adjusted. In principle, the model described in the previous section could be used to more accurately describe the imploding load. However, the transit time of the load can be short compared with that of the PFS so the use of the numerically simpler model is warranted for the purposes of this study.

Three cases have been run for comparison. In case (a) the transit time of the PFS, τ , is held fixed at 100 ns. In this case the energy stored in the inductor L_0 is prevented from being rapidly extracted to implode the load. In case (b) the transit time of the PFS is held fixed at 5 ns. Here the stored energy can be rapidly released to drive the load. In case (c) $\tau_1(t)$ decreases linearly from 100 ns to 5 ns in ~ 200 ns. This models the actual situation for a PFS. Results from these three runs are compared in Figs. 6, 7, 8 and 9. In Fig. 6 $\tau_1(t)$ is plotted for the three cases. In Fig. 7 the load current is plotted, and in Figs. 8 and 9 the total load energy and radius of the imploding load are plotted. The code runs terminate, and therefore the curves end, when the imploding load reaches one tenth of its original radius. Because of the

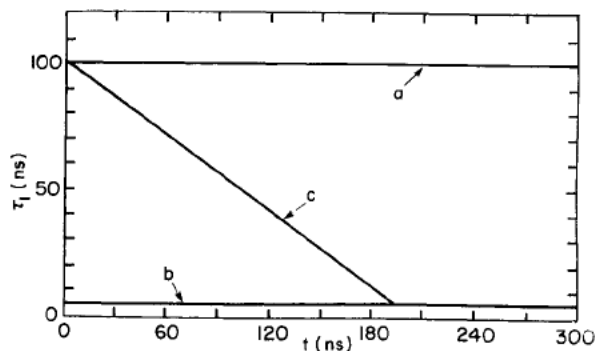


Fig. 6 Plot of $\tau_1(t)$ for cases (a), (b) and (c).

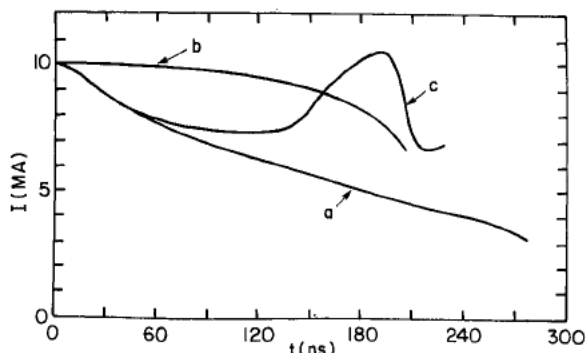


Fig. 7 Load current for cases (a), (b) and (c).

proximity of the load to the large storage inductor in case (b), the load current is maintained at a high value and energy is readily extracted from the store. In case (a), however, the current drops as energy is expended to drive the load inward. Because of the 100 ns transit time, energy is supplied to the load very slowly. In case (c), which models the PFS, the current initially drops as in case (a) when $\tau_1 \sim 100$ ns. As τ_1 decreases, however, the current begins to increase and energy is rapidly released to the load as indicated in Fig. 8. The current actually overshoots the current in case (b) because of LC ringing in the simple circuit chosen to model the problem. The finite capacitance of the element modeling the PFS allows charge to accumulate as voltage is generated by the imploding load. At early time $\omega \sim (L_0 C_1)^{-1/2}$ is small but, as the transit time of the PFS element decreases, ω increases. When τ_1 reaches 5 ns, the period of the ringing has decreased to $T = 2\pi/\omega \sim 10^{-7}$ s close to what is observed. More importantly energy is released rapidly from the storage inductor to drive the load as illustrated in Fig. 9. The radius of the imploding load is also shown in Fig. 9 for comparison of the three cases. Initially the radius in case (c) follows closely to that in case (a). As the transit time decreases, however, the implosion speed rapidly increases reaching nearly the same speed as case (b) at the end of the implosion.

IV. Summary

Models for both the PFS run-down and opening have been presented. These models were incorporated into a transmission line code and were used in simple circuits to demonstrate properties of PFS operation including commutation and load dynamics. A more accurate treatment of the changing transit time of the PFS during commutation using approximate

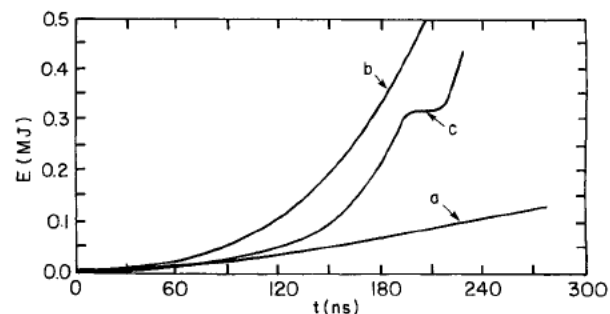


Fig. 8 Total load energy for cases (a), (b) and (c).

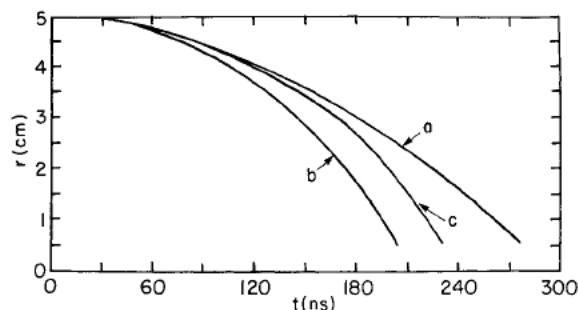


Fig. 9 Imploding load radius for cases (a), (b) and (c).

acoustic analysis will be the next improvement. In the future these models will be used in more sophisticated circuits for comparison with experimental results and for designing new experiments.

V. Acknowledgements

This work was supported by DNA. The authors also wish to acknowledge valuable discussions with R.J. Comisso, D.D. Hinshelwood, J. Neri, J.M. Grossmann and G. Cooperstein.

VI. References

1. P.J. Turchi, G. Bird, C. Boyer, D. Conte, J.F. Davis, L. DeRaad, G. Fisher, L. Johnson, A. Latter, S. Seiler, D. Thomas, W. Tsai and T. Wilcox, "Development of Coaxial Plasma Guns for Power Multiplication at High Energy," in *Proceedings of the Third IEEE Pulsed Power Conference*, June 1981, p. 455.
2. P.J. Turchi, "Magnetoacoustic Model for Plasma Flow Switching," in the *Proceedings of the Fourth IEEE Pulsed Power Conference*, June 1983, p. 342.
3. S. Seiler, J.F. Davis, P.J. Turchi, G. Bird, C. Boyer, D. Conte, R. Crawford, L. DeRaad, G. Fisher, A. Latter, W. Tsai and T. Wilcox, "High Current Coaxial Plasma Gun Discharges through Structured Foils," in *Proceedings of the Fourth IEEE Pulsed Power Conference*, June 1983, p. 346.
4. D.D. Hinshelwood, "BERTHA - A Versatile Transmission Line and Circuit Code," Naval Research Laboratory Memorandum Report 5185, November 1983.
5. D.D. Hinshelwood, private communication.